CONTRIBUTED
P A P E R

Atmospheric Media Calibration for the Deep Space Network

Automatic calibration systems have been developed for tracking spacecraft on inter-planetary missions; the systems account for communication delays due to atmospheric effects.

By Yoaz E. Bar-Sever, Christopher S. Jacobs, Stephen Keihm, Gabor E. Lanyi, Charles J. Naudet, Hans W. Rosenberger, Thomas F. Runge, Alan B. Tanner, and Yvonne Vigue-Rodi

ABSTRACT | Two tropospheric calibration systems have been developed at the Jet Propulsion Laboratory (JPL) using different technologies to achieve different levels of accuracy, timeliness, and range of coverage for support of interplanetary NASA flight operations. The first part of this paper describes an automated GPS-based system that calibrates the zenith tropospheric delays. These calibrations cover all times and can be mapped to any line of sight using elevation mapping functions. Thus they can serve any spacecraft with no prior scheduling or special equipment deployment. Centimeter-level accuracy is provided with 1-h latency and better than 1-cm accuracy after 12 h, limited primarily by rapid fluctuations of the atmospheric water vapor. The second part describes a more accurate line-of-sight media calibration system that is primarily based on a narrow beam, gain-stabilized advanced water vapor radiometer developed at JPL. We discuss experiments that show that the wet troposphere in short baseline interferometry can be calibrated such that the Allan standard deviation of phase residuals, a unitless measure of the average fractional frequency deviation, is better than 2×10^{-15} on time scales of 2000 to approximately 10 000 s.

KEYWORDS | Calibrations; Deep Space Network (DSN); GIPSY; GPS; interplanetary; navigation; spacecraft; troposphere; very long baseline interferometry (VLBI); water vapor radiometer (WVR)

Manuscript received January 22, 2007; revised May 9, 2007. This work was supported by the National Aeronautics and Space Administration.
The authors are with the Jet Propulsion Laboratory, California Institute of Technology, Pasadena, CA 91109 USA (e-mail: Yoaz.E.BarSever@jpl.nasa.gov; Chris.Jacobs@jpl.nasa.gov; Steve.Keihm@jpl.nasa.gov; Gabor.E.Lanyi@jpl.nasa.gov; Charles.J.Naudet@jpl.nasa.gov; Hans.Rosenberger@jpl.nasa.gov; Thomas.F.Runge@jpl.nasa.gov; Alan.Tanner@jpl.nasa.gov; Yvonne.Vigue-Rodi@jpl.nasa.gov).

Digital Object Identifier: 10.1109/JPROC.2007.905181

I. INTRODUCTION

The delays experienced by radiometric signals due to refractive index variations in the Earth's troposphere can be a limiting error source in spacecraft tracking, very long baseline interferometry (VLBI), and radio science applications. Detailed studies of present-day operational spacecraft tracking techniques (Doppler, range, and VLBI) indicate that the uncalibrated troposphere delay is a major source of astrometeric error [1]. Radio science experiments, such as the Cassini gravitational wave experiment, that involve signal propagation between Earth and the spacecraft will be affected by the tropospheric phase fluctuations and require accurate calibration [2]. VLBI astrometric measurements indicate that the coherence time of observations is limited and the delay-rate is dominated by the phase fluctuations induced by the Earth's troposphere [3], [4]. To address these tropospheric errors, the Jet Propulsion Laboratory (JPL) has developed two troposphere calibration systems using different technologies to serve different levels of need for accuracy, timeliness, and range of coverage.

Section II describes an automated GPS-based system that calibrates the zenith troposphere to support Deep Space Network (DSN) tracking of NASA-JPL interplanetary spacecraft. These calibrations cover all times and can be mapped to any desired line of sight using appropriate elevation mapping functions. Thus they can serve any DSN user without requiring any prior scheduling or special equipment deployment. They provide centimeter-level zenith-equivalent accuracy with 1-h latency and better than 1-cm accuracy after 12 h, limited primarily by the inhomogeneous distribution and rapid fluctuations of the atmospheric water vapor.

Section III describes a complementary system for calibrating the fluctuating line-of-sight wet delay using

JPL's advanced media calibration system (MCS). This system is composed of surface metrological equipment, a microwave temperature profiler (MTP), and a water vapor radiometer (WVR). At radio frequencies, the refractivity fluctuations due to water vapor are significantly larger than for hydrostatic air. Due to high refractivity fluctuations and inhomogenous distribution in the atmosphere, water vapor is primarily responsible for the tropospheric phase fluctuations. The thermal emission from the tropospheric water vapor may be measured along a given line of sight on the sky by a water vapor radiometer [5]. These WVR measurements along with other MCS data can be used to deduce the time-dependent delay along the same line of sight, potentially improving the accuracy of spacecraft tracking, radio science measurements, and the coherence of high-frequency VLBI [6]–[9]. To support the Cassini project radio science experiments, JPL developed a narrow-beam gain-stabilized advanced water vapor radiometer optimized to calibrate the tropospheric fluctuations with high accuracy on the timescales of 100–10 000 s. This system can be deployed in advance for the most demanding DSN applications in order to obtain the most precise calibrations possible at cost of increased latency in delivery of the calibration.

II. ZENITH TROPOSPHERE CALIBRATION SYSTEM

NASA's Deep Space Network supports tracking and navigation of an ever-increasing number of interplanetary spacecraft: 15 to 20 are presently being tracked. All of these require reliable, low-cost calibrations for the delay experienced by spacecraft tracking signals due to variable tropospheric refraction, typically with centimeter-level zenith-equivalent accuracy, in order to reduce the effect of this potentially limiting source of error in spacecraft trajectory determination [10]. Spacecraft near planetary encounters or trajectory correction maneuvers often impose a further requirement for latency time of one day or less.

In response to these needs, JPL has developed an automated system that uses Global Positioning System (GPS) data and the JPL GIPSY-OASIS II software[1] to create continuous calibrations of the zenith troposphere delay (ZTD) at the DSN tracking sites in Goldstone, CA; Madrid, Spain; and Tidbinbilla, Australia. Users can then map the zenith calibrations to their lines of sight using appropriate elevation mapping functions [11].

The accuracy of ZTDs derived from GPS data depends strongly on the accuracy of the GPS orbit and clock parameters, which in turn depends on the quality and global distribution of the available GPS data from the ground tracking network. Therefore, GPS orbits and clocks and ZTD data derived from the earliest available GPS data are generally less accurate than products created later when a better selection of GPS data is available. This system extends previous work done at JPL [1] by utilizing real time and rapid service GPS orbit and clock products to provide centimeter-level ZTD accuracy with 1-h latency and subcentimeter accuracy with 12-h latency.

A. Data Processing Description

ZTD estimates for the DSN tracking sites are derived with two cadences: hourly, which creates the most prompt ZTD data possible, and daily, which creates more accurate data with longer latency. Both the hourly and daily processes estimate the ZTD every 5 min at each tracking site.

Both the hourly and daily ZTD estimation processes use JPL's precise point positioning Kalman filter approach [12], which allows rapid determination of a site's position, clock, and tropospheric delay parameters using previously determined GPS orbits and clocks. Dual-frequency GPS phase measurements are selected once every 5 min and are also used to smooth the GPS pseudorange measurements to the 5-min mark. The site position is estimated daily as a constant. The receiver clock is modeled as a white-noise process with updates at every measurement epoch. The zenith tropospheric delay is modeled as a random walk with unconstrained a priori and is mapped in elevation using the Niell hydrostatic, or dry, mapping function. A two-parameter delay gradient is also estimated as a random walk process [13]. The stochastic properties for the ZTD and gradient parameters were derived to optimize position repeatability for a large set of sites. An elevation angle cutoff of 7.5° is used to limit multipath errors while providing enough low-elevation data to extract the gradient parameters [13].

GPS data are collected from the global tracking network operated by member organizations of the International Global Navigation Satellite Systems Service (IGS) as they become available. Not all sites are providing data in time for the hourly or daily processes. All DSN sites, however, are providing GPS data in real time. The hourly process uses the last 6 h of GPS data from the DSN sites with real time GPS orbit and clock products produced by the NASA Global Differential GPS (GDGPS) System.[2] The hourly ZTD estimates are accurate at the 1-cm level rms (less than 0.5% of the DSN zenith path delays, which range from 2.04 to 2.42 meters) and are available within one hour.

The daily solution uses global GPS data covering a 30-hour span centered on noon of each day to minimize data edge effects. Data from some sites are available within minutes while others are not available until hours later. This process begins automatically when a 45-site network with sufficient data quality and global distribution becomes available and typically completes 12 hours after the end of the day. The network data are used to estimate Rapid

[1]http://www.gipsy.jpl.nasa.gov/orms/goa/index.html.

[2]http://www.gdgps.net/.

Service GPS orbit and clock parameters [10], which are then fixed in the DSN site ZTD solutions. The daily ZTD estimates are accurate to better than 1 cm rms.

Next, DSN barometric pressure data are used to separate the ZTD data into *wet* and *dry* (hydrostatic) components. The hydrostatic delay is caused by the induced dipoles in all atmospheric gases and the wet delay is caused by the permanent dipole of water vapor. The Niell hydrostatic and wet mapping functions [11], shown in Figs. 1 and 2, are used to map the zenith delay to the desired elevations. The hydrostatic component typically accounts for about 90% of the total delay and is highly predictable based on the surface pressure, while the wet delay, although relatively small, is highly variable and unpredictable. The zenith hydrostatic (commonly referred to as "dry") delay is determined to better than 2 mm rms by the pressure data, which are accurate to 0.3 mbar rms [5], [14]. The hydrostatic (dry) delays are adjusted from the altitude of the barometer to the altitude of the GPS antenna (see, e.g., [15]) and subtracted from the ZTD to obtain the wet delays. The dry delays are then readjusted to the altitude of the local 70-m antenna, which is the reference height for the calibrations.

Finally, polynomials are fitted to the zenith wet and dry delay time series to facilitate interpolation in time. Each polynomial applies to a specific site and time span (typically 6 h). The fits employ overlapping data spans to reduce edge effects, and collectively cover all times at each DSN site. The rms postfit residuals are typically 0.5–1.0 mm for the wet delay and 0.2–0.5 mm for the dry delay, as illustrated in Fig. 3. These are insignificant since they add in quadrature with the larger estimation errors.

The last two steps are done just before the calibrations are delivered in order to include the most recent data possible. All available ZTD data are processed into calibrations at that time. The hourly data that are used one day are superseded by new daily data the next day, and the affected calibrations are recalculated.

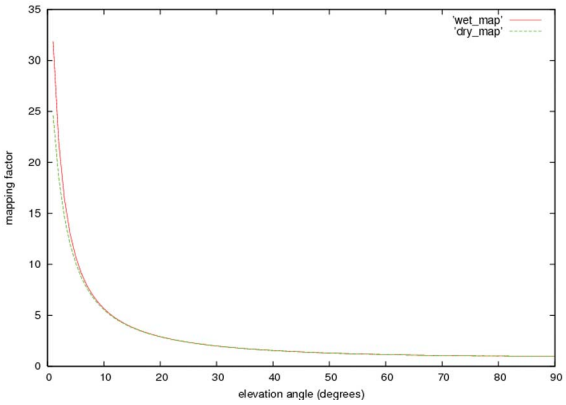

Fig. 1. *Niell wet and dry mapping functions.*

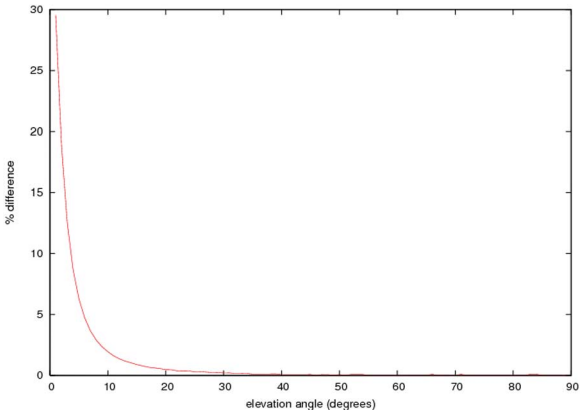

Fig. 2. *Wet–dry mapping percent difference.*

B. Results

Due to the delivery latency requirements, the DSN zenith tropospheric delay estimates are based on GPS orbit and clock parameters determined from a subset of the IGS worldwide GPS receiver data. However, allowing for a latency of about 14 d, one can also estimate the tropospheric delays based on the definitive IGS orbit and clock parameters. A reasonable consistency check of the accuracy of the DSN ZTD estimates is their level of agreement with estimates of tropospheric ZTD based on the definitive IGS orbit and clock products. The IGS ZTD estimates have been shown to be in agreement with WVR measurements at the level of 5 mm [16].

Fig. 4(a)–(c) shows the daily ZTD estimates and the IGS final product for 22 days from March 22 through April 12, 2007, at the three DSN tracking sites. Table 1 lists statistics of the point-by-point differences for each site; the rms difference is less than 5 mm in all cases.

Fig. 5(a)–(c) shows the DSN hourly ZTD estimates and the IGS final product for three days from March 26 through March 28, 2007. (Unfortunately, the hourly estimates are not routinely saved after they are superseded by the subsequent daily estimates.) Table 2 lists statistics of the point-by-point differences; the rms difference is well below 1 cm in all cases. These results are consistent with the expected differences between JPL Rapid Service orbits and clocks and JPL GDGPS orbits and clocks [17].

Another indicator of the precision of the daily ZTD estimates is the difference between successive days' estimates of the ZTD at the day boundary. Table 3 lists the rms ZTD "day jump" for each DSN site for the year 2006.

C. Summary for Section II

High-quality GPS-based ZTD estimates are derived at both hourly and daily intervals in support of flight operations for the Deep Space Network. The use of real-time and rapid service GPS orbit and clock products

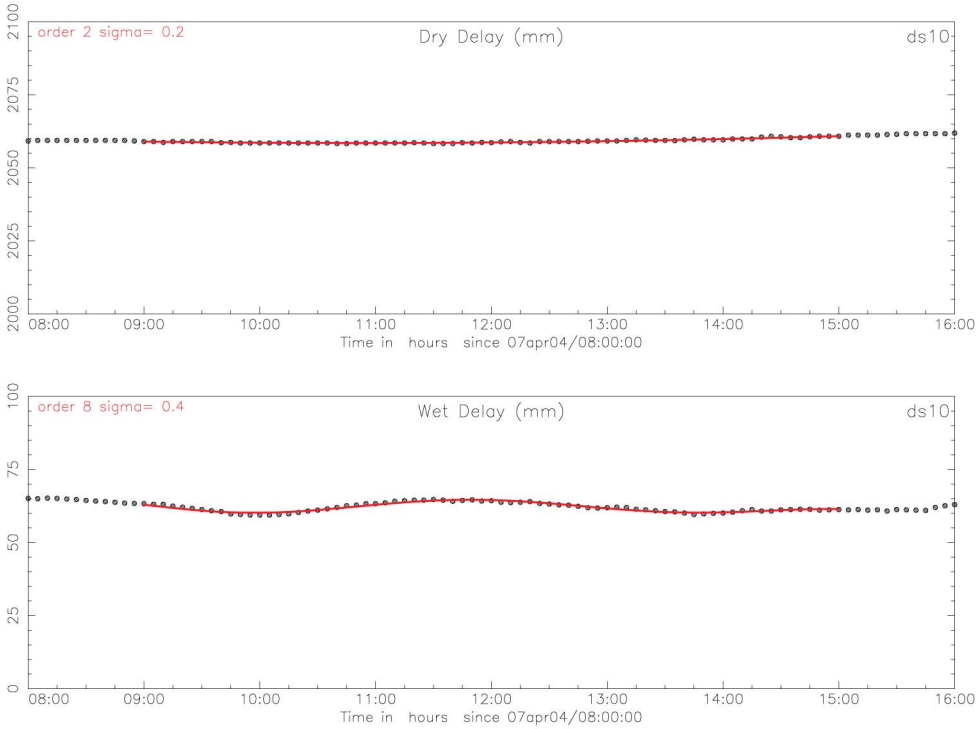

Fig. 3. ***Wet and dry delay calibration fits; the order of the polynomial fit and the standard deviation of the (zero-mean) postfit residual (in millimeters) appear at the upper left of each plot. "ds1" is a pseudonym for Goldstone.***

permits centimeter-level ZTD accuracy with 1-h latency and subcentimeter accuracy after 12 h.

III. THE CASSINI MEDIA CALIBRATION SYSTEM

JPL developed an advanced MCS to support the Cassini radio science experiments. The Cassini spacecraft was launched in 1997 and arrived at Saturn in 2004. Radio science experiments were performed during its cruise phase (early 2001). The Cassini gravitational wave experiment (GWE) has been described in detail by Armstrong [18] and Tinto and Armstrong [2]. Detailed studies of the GWE error budget [19], [20] pointed to atmospheric delay fluctuations as the dominate error component on time scales greater than 100 s. Thus the sensitivity of the GWE was limited by the ability to calibrate out atmospheric delay fluctuations. Since almost all the power in the atmospheric delay fluctuations at frequencies less than 0.01 Hz is due to the water vapor, the principle instrumentation used for calibration is a water vapor radiometer.

An advanced water vapor radiometer, shown in Fig. 6, was developed at JPL and is described in detail by Tanner [21]. Off to the right in the background of Fig. 6 one can see the microwave temperature profiler. The microwave temperature profiler retrieves the vertical distribution of atmospheric temperature. Not shown are surface sensors for temperature, pressure, and relative humidity, which add further constraints to the path delay retrieval processing.

The WVR has an off-axis reflector, providing a 1° beamwidth with very low side lobes. The pointing accuracy is 0.1°. The WVR acquires data in subsecond intervals and produces a time series of line-of-sight brightness temperatures at three frequency channels: the 22.2-GHz water vapor line center is supplemented by frequency channels at 23.8 and 31.4 GHz. The 23.8-GHz channel mitigates the sensitivity of the wet delay measurement to height (pressure) dependencies of the water vapor emission. The 31.4-GHz channel measurement constrains the emission effects due to liquid water clouds when present. The wet path delay along the line of sight is determined from the WVR, MTP, and surface meteorology measurements using one of two retrieval algorithms. A direct inversion Bayesian algorithm [22] is used for clear conditions. A slightly less accurate statistical retrieval algorithm [23] is used when clouds are present. Both algorithms utilize a modification of the Liebe and Layton 1987 model [24] for 20–32 GHz atmospheric water vapor emission. The model validation is based on WVR intercomparisons with radiosondes [25] and GPS [26] and is described in detail in [26].

The objective of the Cassini media calibration system was to measure the atmospheric path delay fluctuation of

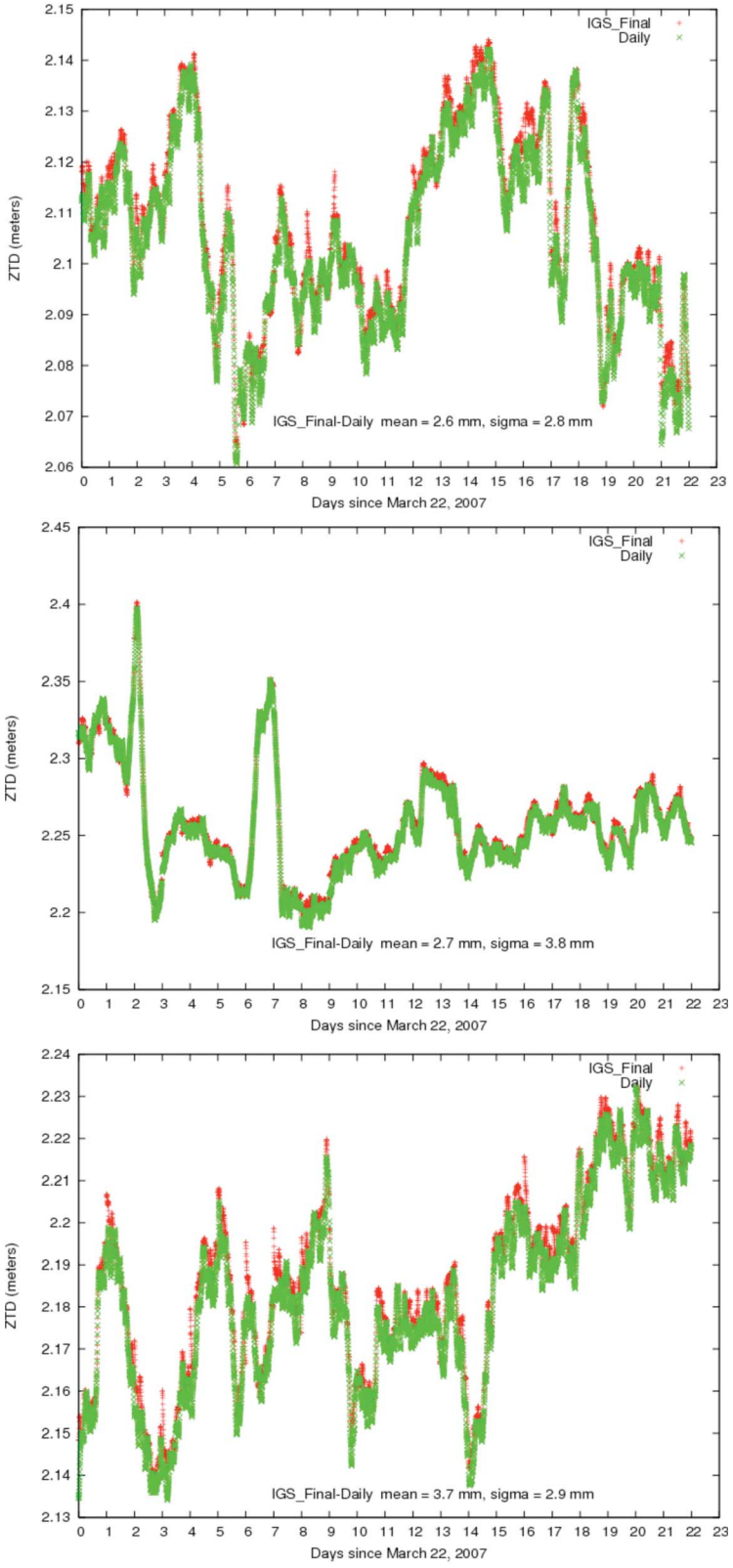

Fig. 4. ***Daily ZTD versus IGS final: (top) Goldstone, (middle) Tidbinbilla, and (bottom) Madrid.***

Table 1 Difference Statistics, Daily ZTDs—IGS Final

Site	Npts	Mean (mm)	Sigma (mm)	RMS (mm)
Goldstone	6263	-2.63	2.78	3.83
Tidbinbilla	5956	-2.73	3.85	4.72
Madrid	6271	-3.65	2.95	4.70

signals transmitted between the Cassini spacecraft and the Goldstone Deep Space Station 25 (DSS-25) antenna. Two advanced WVRs were built to support Cassini radio science experiments. Dual WVRs allow for operational reliability and robustness in case of equipment failure and allow crosschecks between the units. A detailed intercomparison between the two units has been made [27], and the Allan standard deviation [28] was shown to be significantly better than the GWE requirements for all interval times greater than 100 s up to 10 000 s. Full details of the successful calibration of the Cassini gravitational wave experiment can be found elsewhere [29]. In this paper, we will discuss the contribution of the MCS calibration to the precision of connected element interferometry (CEI) and intercontinental VLBI. A detailed description of the VLBI technique used at JPL can be found in [30].

A. MCS Calibration of CEI Measurements

To study in detail the performance of the MCS, a series of comparison experiments utilizing a connected element interferometer were used to independently measure the line-of-sight path delay fluctuations. An overview of the experimental setup is shown in Fig. 7. From August 1999 until May 2000, we conducted a series of dual-frequency (2.3 and 8.4 GHz) CEI observations on a 21-km baseline between the DSN's high-efficiency 34-m-diameter antenna at DSS-15 and a 34-m-diameter beam waveguide antenna at DSS-13. Since the effective wind speed is typically 5–10 m/s or less, the tropospheric fluctuations at each site are independent for timescales less than ~4000 s, making this baseline well suited for a CEI–MCS comparison experiment. Strong, point-like quasar radio sources (flux density > 1 Jy) with accurately known positions were chosen to minimize CEI errors.

The CEI data (voltage time series) from each antenna were cross-correlated and the interferometric delay (difference in arrival times at the two antennas) extracted. After subtraction of an a priori model, the residual phase delay (residual phase divided by the observing frequency) and delay rate (time rate of change of phase delay) were obtained. The VLBI data include a differential (between the two receiving stations) clock-like term that was removed by statistical estimation [31]. This procedure also removed the part of the differential zenith tropospheric delay that is linear with respect to time.

Each WVR was positioned ~50 m from the base of the 34-m antenna. This offset was chosen to maximize the sky coverage while minimizing the magnitude of beam-offset errors [32], [33]. The WVRs were co-pointed with the DSN antennas during sidereal tracking of distant natural radio sources. The MCS data was monitored in real time, and derived path-delay time series were produced during postprocessing. After the WVR path delay time series were smoothed over 6-s intervals, the WVR data from each site (DSS-15, DSS-13) were subtracted to create a site-differenced delay time series. Finally, to make it identical to the VLBI observables, the linear part of the differential delays was removed, resulting in a differenced WVR data type that could be directly compared with the CEI residual phase delays.

The comparison experiments conducted in 1999 were limited in scan duration to less than 26 min (the duration of a single pass on the CEI tape recorder). Several experiments produced little data, due to an assortment of instrumental problems and operator errors. In addition, instrumental problems at DSS-13 caused uncalibrated delay errors on long (> 1000 s) timescales. A fairly representative experiment is day-of-year (DOY) 240, 2000. This experiment consisted of 11 scans, each of duration ~26 min covering a wide variety of azimuths and elevations. For ease of comparison between data sets at different elevations, both the CEI and WVR data sets have been converted (mapped) to the equivalent delays in the zenith direction.

A time series of the site-differenced residual phase delay for both the CEI and WVR data for scan 3 is shown in Fig. 8. It is clear that the correlation between the two data sets is strong. The CEI data can be calibrated for phase delay fluctuations by subtracting the corresponding WVR data. Figs. 9 and 10 plot the residual path delay histogram of DOY 240 for the CEI data before and after calibration, respectively. Before calibration, the rms is ~1.1 mm; after calibration, it is 0.42 mm. Thus an improvement by a factor of approximately three is seen.

By May 2000, we were able to upgrade the frequency distribution system at DSS-13, correcting the long-term CEI instrumental stability problems, enabling WVR-CEI comparison over very long timescales (> 1000 seconds). Two experiments, DOY 137 and DOY 138, were conducted after these long-term stability problems were corrected. The CEI and WVR delay time-series data from DOY 138 are shown in Fig. 11. The CEI and WVR residual path delay data sets track very closely. The CEI data have an rms of ~4.3 mm. After WVR calibration, this is reduced to ~1 mm, a factor of four improvement. On DOY 137, an improvement factor of 1.7 was measured; however, surface

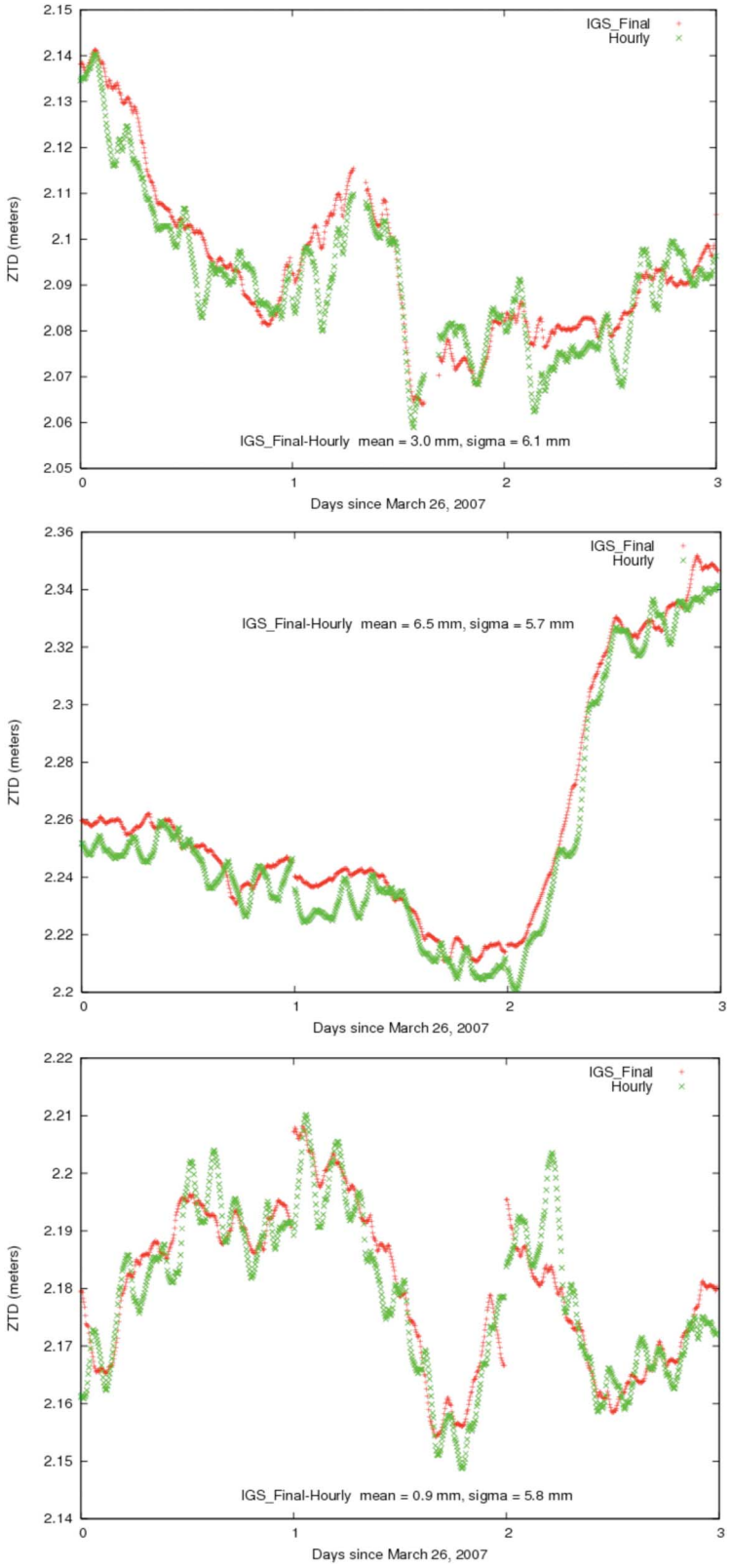

Fig. 5. ***Hourly ZTD versus IGS final: (top) Goldstone, (middle) Tidbinbilla, and (bottom) Madrid.***

Table 2 Difference Statistics, Hourly ZTDs—IGS Final

Site	Npts	Mean (mm)	Sigma (mm)	RMS (mm)
Goldstone	823	-3.02	6.07	6.77
Tidbinbilla	858	-6.48	5.70	8.63
Madrid	858	-0.88	5.75	5.81

Table 3 2006 DSN ZTD Day Jumps

Site	RMS
Goldstone	2.59 mm
Tidbinbilla	5.34 mm
Madrid	2.84 mm

winds were measured to be in excess of 40 km/h. At this level of surface wind, the antenna pointing error along with turbulent dry delay are the chief suspects for diminished performance.

Fig. 12 plots the Allan standard deviation (ASD)[3] of the site-differenced delays as a function of the sampling time for DOY 138. The CEI data and WVR data have ASD values that track one another very closely over almost the entire range of sampling times. After the WVR data are used to calibrate the CEI data for atmospheric media delay, the ASD decreases by a factor of six at time intervals of 1000 s. The calibrated CEI data show improvement for all sampling times down to ~15 s, below which the 50-m WVR-DSN offset limits useful calibration.

The solid black curve in Fig. 12 is the Cassini GWE ASD requirement. For sampling times above 2000 s, the MCS performance, as indicated by the calibrated CEI data, matches the Cassini requirements. Below sampling times of 1000 s, the MCS performance fails to reach the requirements by a factor of two to three. Unknown CEI errors and the 50-m beam offset are believed to be the cause of performance discrepancy for time scales of 100–1000 s.

The CEI–MCS comparison data discussed so far is but a small sample of the data collected. More than 30 CEI–MCS comparison experiments were conducted between August 1999 and May 2000. Not all of the CEI experiments showed residual scatter improvement of factors of three or better after media calibration; approximately 15% of the experiments resulted in improvements of factors between one and three. These experiments largely correlated with misty and rainy weather conditions. Previous papers describe the full details of the instrumentation, observing strategy, data analysis procedures, weather conditions, error budgets, and performance evaluation [34]–[36].

[3]The Allan variance is defined as the square phase deviation of each sample from the mean of its two adjacent samples [28]. The reference frequencies used were 8.41×10^9 Hz (X-band) and 32.1×10^9 Hz (Ka-band) for the CEI and VLBI data, respectively.

Fig. 6. *A photo of the Cassini Media Calibration Subsystem taken at DSS-13 in Goldstone, CA. The new advanced WVR is seen in the center and the MTP and J-series WVR are shown in the background to the right. The WVR antenna is a 1-m-diameter offset parabolic reflector with a 1° beamwidth.*

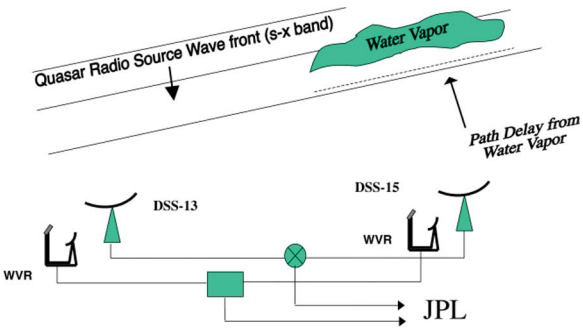

Fig. 7. *A schematic representation of the WVR/CEI comparison experimental setup.*

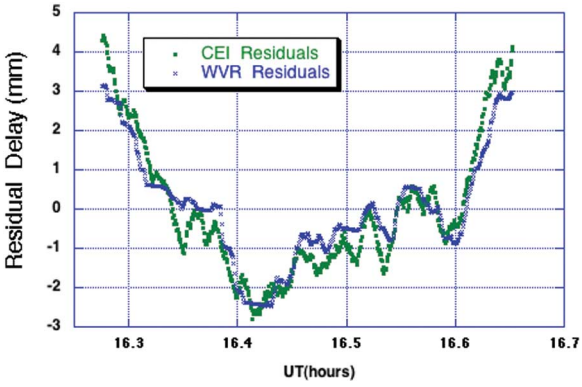

Fig. 8. *The site-differenced zenith-mapped residual delay data from the CEI and WVR for scan 3 on DOY 240, 1999.*

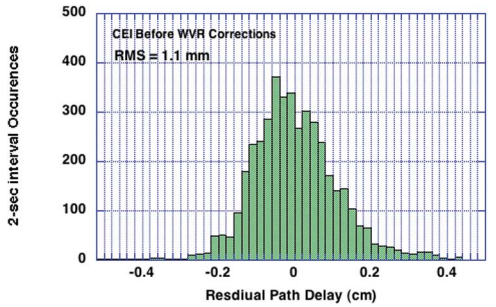

Fig. 9. *Histogram of the residual path delays for the uncalibrated CEI data from all scans on DOY 240, 1999. RMS = 1.1 mm.*

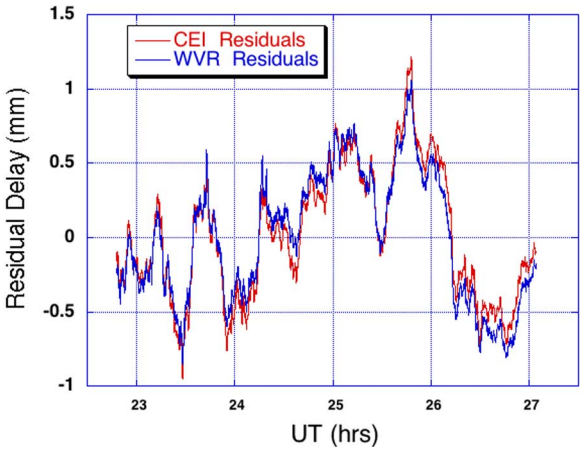

Fig. 11. *The residual delay measured by the CEI and WVR for a long scan on DOY 138, 2000. The data is site-differenced, mapped to zenith, and with linear trends removed.*

B. MCS Calibration of VLBI Measurements

Following the successful calibration support of the Cassini gravitation wave experiment, one MCS was moved to the Deep Space Network Madrid complex and installed near DSS55, the DSN's 34-m beam waveguide antenna [37]. The installation was optimized to support calibrations for intercontinental VLBI measurements between Madrid and Goldstone. The accuracy of VLBI global astrometry has long been known to be limited by systematic errors, principally stochastic fluctuations of the refractive delay caused by atmospheric water vapor. Reducing this error component has the potential to improve the overall VLBI astrometric observations, which are used to construct global reference frames such as the International Celestial Reference Frame [38]. These reference frames are an essential component of modern deep-space navigation.

The results described below are from two intercontinental VLBI observing sessions done during the summer of 2004 using DSS-26 in Goldstone California and DSS-55 near Madrid. The first session was on DOY 200 (July 18, 2004) and the second session was on DOY 217 (August 4, 2004). The experimental setup was nearly identical to that of the earlier discussed CEI experiments (Fig. 7), the differences being a much longer intercontinental baseline and improvements in the hardware and postprocessing software that were used. We recorded VLBI data simultaneously at X- (8.4 GHz) and Ka-band (32 GHz), sampling each band at a rate of 64 Mbps. The data were sampled, digitally filtered, and recorded to hard disk using the JPL-designed VLBI science receivers. The data were played back over a network connection and then correlated with the SOFTC software correlator [39]. Fringe fitting was done with the FIT fringe fitting software [31]. This procedure resulted in a phase delay measurement for each second of an hour-long scan. The observed elevations were moderate, ranging from roughly 30 to 50°, as seen in Table 4.

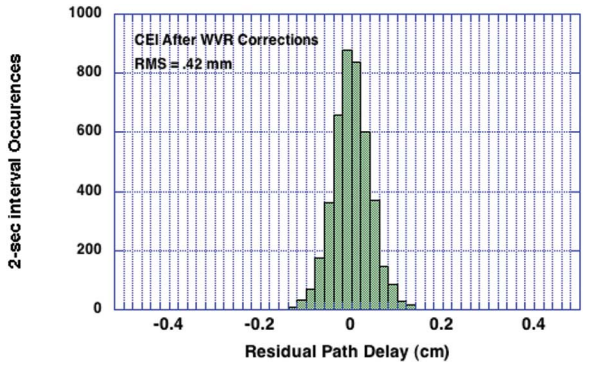

Fig. 10. *Histogram of the residual path delay for the calibrated CEI data from all scans on DOY 240, 1999. The CEI data after WVR correction have an rms = .42 mm.*

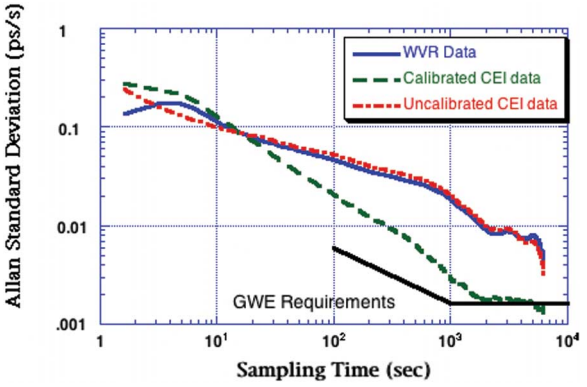

Fig. 12. *The Allan standard deviation plotted as a function of sampling time for the long scan of DOY 138, 2000. The figure shows the CEI residual data, the WVR residual data, the CEI data after WVR corrections, and the requirements for the Cassini GWE.*

Table 4 The Average Antenna Elevation, in Degrees, at Both DSN Antenna Sites at Both Beginning and End of the Experiment on Day of Year (DOY) 200 and 217

Time	Elevations (deg)	
DOY/hh:mm	DSS 26 (Goldstone)	DSS 55 (Madrid)
200/10:00	31.7	53.3
200/11:00	43.7	41.9
217/09:00	33.0	52.0
217/10:00	45.0	40.6

The experimental data obtained on DOY 200 and 217 are shown in Figs. 13 and 14, respectively. Both clearly show that even over intercontinental baselines, a very high correlation exists between the VLBI residual phase delay and the WVR-measured troposphere calibrations. After WVR calibration, the improvement in residuals is almost a factor of three for both time series. For example, the DOY 200 VLBI phase residuals improved from 3.4 to 1.2 mm, a factor of 2.8 improvement.

In order to examine the range of time scales over which the VLBI residuals are being improved, we calculated the Allan standard deviation of the VLBI delays. Fig. 15 shows the Allan standard deviation from sample times of 10–1800 s for the VLBI data on DOY 200, 2004 before (red) and after (green) the WVR calibration. The result shows a strong improvement on time scales of 10–1800 s; the calibrated VLBI data have improved by a factor of three. For times scales shorter than 10 s, we note that low WVR SNR forced its shortest measurement integrations to be ~10 s, which contributed to the lack of significant improvement on time scales less than 10 s. The DOY 200 and 217 experiments only lasted 3600 s, thus limiting our ability to examine the quality of calibrations on time scales much longer than 1000 s.

There is a suggestion in the data of Figs. 13 and 14 that the WVR does not track some sharp peaks in the VLBI phase delay. The wider beam of the WVR (1°) relative to the VLBI antenna (0.02° at Ka-band 32 GHz) and the spatial offset of the two instruments (on the order of 100 m) are potential contributors to this effect.

Noting that these tests probed only time scales on the order of 10–1000 s and because global VLBI passes often last for 24 h, one would like to demonstrate that the WVR calibrations reduce VLBI residuals on time scales out to a day (~100 000 s). Also, these measurements represent one continuous track of a single natural radio source as it moves slowly across the sky. We have not yet demonstrated that the

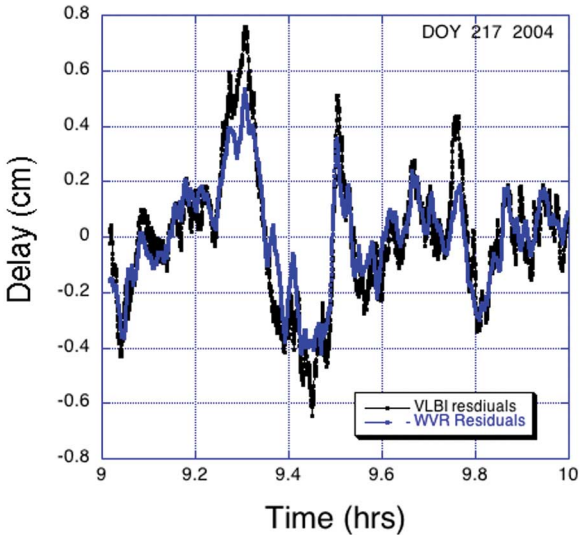

Fig. 14. *VLBI delay residual time series and WVR tropospheric calibration delay residuals for DOY 217, 2004. Ka-band on the DSS-26 and DSS-55 baseline.*

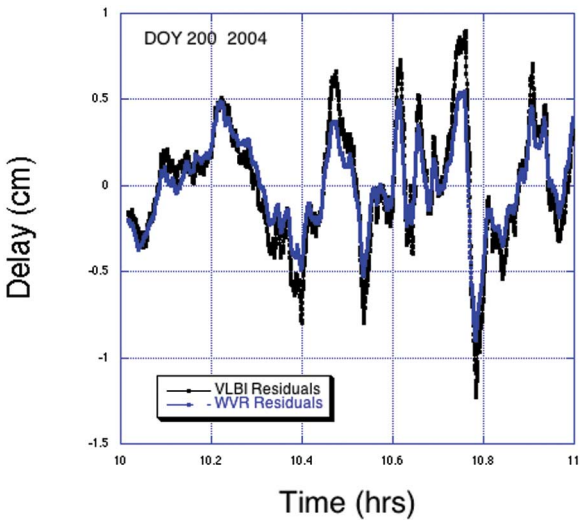

Fig. 13. *VLBI delay residuals time series and WVR tropospheric calibration delay residuals for DOY 200, 2004. Ka-band on the DSS-26 and DSS-55 baseline.*

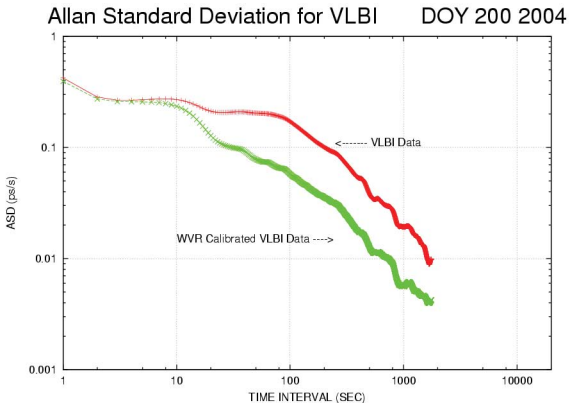

Fig. 15. *Allan Standard Deviation for VLBI data (red) before and (green) after the WVR calibration for time samples from 10 to 1800 s.*

dramatic improvements seen in our data can be sustained in a typical global astrometry scenario in which the target radio source is changed every few minutes to a different part of the sky. Such a demonstration remains for future work.

C. Summary of Section III

We have described an atmospheric media calibration system that was shown to calibrate out the atmospheric delay fluctuations in short baseline CEI experiments down to an Allan standard deviation level of 2×10^{-15} for sampling times from 2000 to approximately 10 000 s. Both the CEI and VLBI experiments show that, after MCS calibration, the measured Allan standard deviation residuals were improved by a factor of two to three for time scales longer than 100 s and the delay residuals were reduced by approximately a factor of three.

The improvements indicate, at least differentially, that a WVR can estimate the water vapor induced propagation delays at the 1 mm level of precision under semidry atmospheric conditions. Consequently, it has the potential of decreasing the error in angular spacecraft position determination measurements. In addition, it would reduce the source of errors in the position of radio sources needed for the angular measurements. Therefore, it would also reduce the amount of time needed to develop an X/Ka-band (8.4/32 GHz) celestial reference frame for applications such as spacecraft tracking. ■

Acknowledgment

The authors are very grateful to L. Skjerve, L. Tandia, J. Clark, the staff at DSS13, and the operations crews at the Goldstone Signal Processing Center for the invaluable assistance they provided during the VLBI experiments; and L. Teitelbaum and R. Linfield for their helpful discussions on data analysis of delay fluctuations.

REFERENCES

[1] C. L. Thornton and J. S. Border, *Radiometric Tracking Techniques for Deep-Space Navigation*. New York: Wiley, 2003.

[2] M. Tinto and J. W. Armstrong, "Spacecraft Doppler tracking as a narrow-band detector of gravitational radiation," *Phys. Rev. D*, vol. 58, p. 042002, 1998.

[3] A. E. E. Rogers, A. T. Moffet, D. C. Backer, and J. M. Moran, "Coherence limits in VLBI obervations at 3-mm wavelength," *Radio Sci.*, vol. 19, pp. 1552–1560, 1984.

[4] R. N. Truehaft and G. E. Lanyi, "The effect of the dynamic wet tropsphere on radio interferometric measurements," *Radio Sci.*, vol. 22, pp. 251–265, 1987.

[5] G. Elgered, "Tropospheric radio path delay from ground-based microwave radiometry," in *Atmospheric Remote Sensing by Microwave Radiometry*, M. Janssen, Ed. New York: Wiley, 1992.

[6] G. M. Resch, D. E. Hogg, and P. J. Napier, "Radiometric correction of atmospheric path length fluctuations in interferometric experiments," *Radio Sci.*, vol. 19, pp. 411–422, Jan. 1984.

[7] A. J. Coster, A. E. Niell, F. S. Solheim, V. B. Mendes, P. C. Toor, K. P. Buchmann, and C. A. Upham, "Measurements of precipitable water vapor by GPS, radiosondes, and a microwave water vapor radiometer," in *Proc. ION-GPS Conf.*, Kansas City, KS, Sep. 17–20, 1996.

[8] D. A. Tahmoush and A. E. E. Rogers, "Correcting atmospheric path variations in millimeter wavelength very long baseline interferometry using a scanning water vapor spectrometer," *Radio Sci.*, vol. 35, pp. 1241–1251, 2000.

[9] A. L. Roy, H. Rottmann, U. Teuber, and R. Keller, *Phase Correction of VLBI with water vapor radiometry*, Mar. 5, 2007, arXiv:astro-ph/0703066v1.

[10] S. M. Lichten, "Estimation and filtering for high-precision GPS applications," *Manuscripta Geodaetica*, vol. 15, pp. 159–176, 1990.

[11] A. E. Niell, "Global mapping functions for the atmospheric delay at radio wavelengths," *J. Geophys. Res.*, vol. 101, no. B2, 1996.

[12] J. Zumberge, M. Heflin, D. Jefferson, M. Watkins, and F. Webb, "Precise point positioning for the efficient and robust analysis of GPS data from large networks," *J. Geophys. Res.*, vol. 102, no. B3, pp. 5005–5017, 1997.

[13] Y. E. Bar-Sever, P. M. Kroger, and J. A. Borjesson, "Estimating horizontal gradients of tropospheric path delay with a single GPS receiver," *J. Geophys. Res.*, vol. 103, no. B3, pp. 5019–5035, 1998.

[14] J. Saastamoinen, *Atmospheric Correction for the Troposphere and Stratosphere in Radio Ranging of Satellites*, ser. The Use of Artificial Satellites for Geodesy, Geophysics Monograph Series. Washington, DC: American Geophysical Union, 1972.

[15] V. de Brito Mendes, "Modeling the neutral-atmosphere propagation delay in radiometric space techniques," Dept. of Geodesy and Geomatics Engineering, Univ. of New Brunswick, Fredericton, NB, Tech. Rep. 199, Apr. 1999, p. 46.

[16] S. H. Byun, Y. E. Bar-Sever, and G. Gendt, "The new troposphere product of the international GNSS service," in *Proc. Inst. Navig. ION GNSS 2005*, Long Beach, CA, Sep. 14–16, 2005.

[17] M. B. Heflin, Y. E. Bar-Sever, D. C. Jefferson, R. F. Meyer, B. J. Newport, Y. Vigue-Rodi, F. H. Webb, and J. F. Zumberge, "JPL IGS Analysis Center report 2001–2003," IGS, 2004.

[18] J. W. Armstrong and R. A. Sramek, "Observations of tropospheric phase scintillations at 5 GHz on vertical paths," *Radio Sci.*, vol. 17, pp. 1579–1586, Nov. 1982.

[19] J. W. Armstrong, B. Bertotti, F. B. Estabrook, L. Iess, and H. D. Wahlquist, "The Galileo/Mars observer/Ulysses coincidence experiment," *Proc. 2nd Edoardo Amaldi Conf. Gravitat. Waves*, vol. 4, E. Coccia, G. Pizzella, and G. Veneziano, Eds., 1998, vol. 4.

[20] S. J. Keihm, "Water vapor radiometer measurements of the tropospheric delay fluctuations at Goldstone over a full year," TDA Prog. Rep. 42-122, 1999, pp. 1–11.

[21] A. B. Tanner, "Development of a high-stability water vapor radiometer," *Radio Sci.*, vol. 33, pp. 449–462, Mar. 1998.

[22] S. J. Keihm and S. Marsh, "New model-based Bayesian inversion algorithm for the retrieval of wet tropospheric path delay from radiometric measurements," *Radio Sci.*, vol. 33, no. 2, pp. 411–419, 1998.

[23] G. M. Resch, "Inversion algorithms for water vapor radiometers operating at 20.7 and 31.4 GHz," TDA Prog. Rep. 42-76, Oct. 1983, pp. 12–26.

[24] H. J. Liebe and D. H. Layton, "Millimeter wave properties of the atmosphere: laboratory studies and propogation modeling," Nat. Telecommun. Inform. Admin., Boulder, CO, NTIA Rep. 87-24, 1987.

[25] S. J. Keihm, *Water Vapor radiometer intercomparison experiment*, Platteville, CO, JPL Doc. D-8898, 1991.

[26] S. J. Keihm, Y. Bar-Sever, and J. C. Liljegren, "WVR-GPS comparison measurements and calibration of the 20–32 GHz tropospheric water vapor absorption model," *IEEE Trans. Geosci. Remote Sensing*, vol. 40, no. 6, pp. 1199–1210, 2002.

[27] S. J. Keihm, A. Tanner, and H. Rosenberger, "Measurements and calibration of tropospheric delay at Goldstone from the Cassini media calibration system," JPL IPN Prog. Rep. 42-158, Aug. 15, 2004, pp. 1–17.

[28] D. W. Allan, "Statistics of atomic frequency standards," *Proc. IEEE*, vol. 54, pp. 221–230, Feb. 1966.

[29] S. Abbate *et al.*, "The Cassini gravitational wave experiment," in *Proc. SPIE Gravitat. Wave Detection*, vol. 4856, M. Cruise and P. Saulson, Eds., 2003, vol. 4856, pp. 90–97.

[30] O. J. Sovers, J. Fanselow, and C. S. Jacobs, "Astrometry and geodesy with radio interferometry: Experiments, models, results," *Rev. Modern Phys.*, vol. 70, no. 4, pp. 1393–1454, Oct. 1998.

[31] S. Lowe, *Theory of Post-block II VLBI observable extraction*, JPL Pub. 92-7, Jul. 15, 1992.

[32] R. P. Linfield and J. Wilcox, "Radio metric errors due to mismatch and offset between a DSN antenna beam and the beam of a tropospheric calibration instrument," TDA Prog. Rep. 42-114, 1993, pp. 1–13.

[33] R. P. Linfield, Error budget for WVR-based tropospheric calibration system, JPL IOM 335.1-96-012, Jun. 5, 1996.

[34] C. Naudet, C. Jacobs, S. Keihm, G. Lanyi, R. Linfield, G. Resch, L. Riley, H. Rosenburger, and A. Tanner, "The media calibration system for Cassini radio science: Part I," TMO Prog. Rep. 42-143, Nov. 15, 2000.

[35] G. Resch, J. Clark, S. Keihm, G. Lanyi, R. Linfield, C. Naudet, L. Riley, H. Rosenburger, and A. Tanner, "The media calibration system for Cassini radio science: Part II," TMO Prog. Rep. 42-145, May 15, 2001.

[36] G. Resch, J. Clark, S. Keihm, G. Lanyi, R. Linfield, C. Naudet, L. Riley, H. Rosenburger, and A. Tanner, "The Media calibration system for Cassini radio science: Part III," IPN Prog. Rep. 42-148, Feb. 15, 2002.

[37] J. Oswald, L. Riley, A. Hubbard, H. Rosenberger, A. Tanner, S. Keihm, C. Jacobs, G. Lanyi, and C. Naudet, "Relocation of advanced water vapor radiometer to deep space station 55," IPN Prog. Rep. 42-163, Nov. 15, 2005.

[38] C. Ma, E. F. Arias, T. M. Eubanks, A. L. Fey, A.-M. Gontier, C. S. Jacobs, O. J. Sovers, B. A. Archinal, and P. Charlot, "The international celestial reference frame as realized by very long baseline interferometry," *Astron J.*, vol. 116, p. 516, 1998.

[39] S. T. Lowe, "SOFTC: A software VLBI correlator," Jet Propulsion Laboratory, Pasadena, CA, JPL Tech. Rep., 2005.

ABOUT THE AUTHORS

Yoaz E. Bar-Sever is Deputy Manager of the Tracking Systems and Applications Section, Jet Propulsion Laboratory, Pasadena, CA, and Manager of the NASA Global Differential GPS System. His technical expertise lies with satellite dynamics modeling, GPS orbit determination, and tropospheric sensing with GPS.

Christopher S. Jacobs received the B.S. degree in applied physics from California Institute of Technology, Pasadena, in 1983.

He is a Senior Engineer with the Deep Space Tracking Systems Group, Jet Propulsion Laboratory, Pasadena. His work has centered on producing quasi-intertial reference frames based on observations of extragalactic radio sources. These frames define the angular coordinates used for spacecraft navigation. He has served on IAU working groups for celestial reference frames as a coauthor of the paper that introduced the extragalactic radio frame (ICRF) as a replacement for optically based definitions of celestial angular coordinates. His recent research interests have focused on extending the ICRF to higher radio frequency bands such as 24, 32, and 43 GHz.

Mr. Jacobs is a member of AAS.

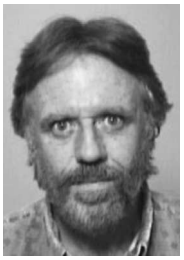

Stephen Keihm received the B.S. degree in physics from Fordham University, Bronx, NY, in 1968, the B.S. degree in mechanical engineering from Columbia University, New York, in 1969, and the M.S. degree in astronautical science from Stanford University, Stanford, CA, in 1970.

From 1970 to 1978, he was a Research Assistant, then Staff Associate, with the Lamont-Doherty Geological Observatory, Columbia University. While with Lamont, he was Co-Investigator for the Apollo 15 and 17 lunar heat flow experiments and Principal Investigator in studies of the thermal and electrical properties of the lunar regolith. In 1978, he joined the Planetary Science Institute, Pasadena, CA, where he conducted theoretical studies for the interpretation of data from the remote sensing of planetary surfaces. Since 1982, he has been with the Jet Propulsion Laboratory, California Institute of Technology, Pasadena, where he has developed lunar calibration models for the Cosmic Background Explorer Experiment, the Microwave Limb Sounder instrument, and the Rosetta Microwave Radiometer instrument. He has also worked extensively in the areas of algorithm development and data interpretation for Earth-based, aircraft, and satellite microwave measurements of the atmosphere and sea surface. Currently, he is Instrument Scientist for the Cassini Radio Science Tropospheric Calibration System and Supervisor of the Ground-Based Microwave Applications Group, JPL.

Gabor E. Lanyi received the Ph.D. degree in physics from Syracuse University, Syracuse, NY, in 1977.

He has been with the Jet Propulsion Laboratory, Pasadena, CA, since 1979, working primarily in the area of astrometry for deep-space tracking applications. His research area also includes refraction effects in terrestrial media, GPS-based ionospheric content determination, weak signal detection, and fundamental laws of physics.

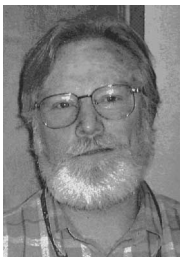

Charles J. Naudet received the B.S. degree in engineering physics from the University of Kansas, Lawrence, in 1979 and the M.S. and Ph.D. degrees in physics from Rice University, Houston, TX, in 1983 and 1986, respectively.

From 1986 to 1993, he was with the Nuclear Science Division, Lawrence Berkeley Laboratory (LBL). While at LBL, he served first as a Postdoctorial Research Assistant, then as a Member of Research Staff studying dielectron production in nucleus-nucleus interactions. In 1993, he joined the Jet Propulsion Laboratory (JPL), Pasadena, CA, as a Member of Technical Staff studying astrometric measurements of quasars and spacecraft. In 1999, he became a Member of Senior Staff and in 2003 Group Supervisor of the Deep Space Tracking Systems Group, JPL. He is Manager of the Interplanetary Network Directorate Radiometrics Technology work area, a Co-Investigator on the VLBA Deep Space Navigation project, and a Co-Investigator on the Antarctic Impulsive Transient Antenna.

Hans W. Rosenberger received the B.A. degree in physics from Goshen College, Goshen, IN, in 1995, the M.S. degree in electrical engineering from Pennsylvania State University, University Park, in 1999, and the M.B.A. degree from the University of Southern California, Los Angeles, in 2006.

He is currently with the Jet Propulsion Laboratory, Pasadena, part-time as a Contractor (Santa Barbara Applied Research). He is contributing to maintenance of the MCS instruments and upgrading the processing software. He was a prime contributor to the software development of the MCS and the system's initial deployment.

Thomas F. Runge received the B.A. degree in mathematics and the Ph.D. degree in computer science from the University of Illinois, Urbana, in 1971 and 1977, respectively.

From 1971 to 1977, he was with the Atomic Energy Commission and later the U.S. Department of Energy, developing a generalized network simulation software package. From 1977 to 1981, he was ith Sandia National Laboratories, Albuquerque, NM, where he developed computerized safeguard systems for nuclear facilities for the Department of Energy. Since 1981, he has been with the Jet Propulsion Laboratory, California Institute of Technology, Pasadena, where he has developed software and operational systems for determining Earth orientation parameters and calibrating media transmission effects on radiometric spacecraft tracking data. He was Task Manager of the DSN TEMPO (Time and Earth Motion Precision Observations) program from 1984 to 1994 and of the DSN Media Modeling program from 1987 to the present. He is currently the DSN Subsystem Engineer for Radiometric Modeling and Calibration.

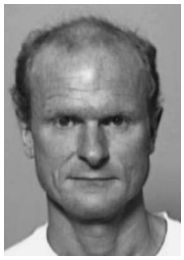

Alan B. Tanner received the B.S. and Ph.D. degrees from the University of Massachusetts at Amherst in 1984 and 1989, respectively.

He is a Microwave Systems Engineer with the Jet Propulsion Laboratory, Pasadena, CA. His work has focused on the design and calibration of radiometers and radar scatterometers for remote sensing.

Yvonne Vigue-Rodi received the B.S. and M.S. degrees in aerospace engineering from the University of Texas at Austin in 1988 and 1990, respectively.

She is currently a member of Engineering Staff with the Orbiter and Radio Metric Systems Group, NASA's Jet Propulsion Laboratory, where she has spent 17 years on research and development for improved understanding of GPS satellite orbit dynamics for Earth science applications.